Proceedings of the 18th International Conference
on Computational and Mathematical Methods
in Science and Engineering, CMMSE 2018
July 9–14, 2018.

The role of the environment in front propagation

Andrea Trucchia[1,2] **and Gianni Pagnini**[1,3]

[1] *BCAM - Basque Center for Applied Mathematics,*
Alameda de Mazarredo 14, E-48009 Bilbao, Basque Country – Spain

[2] *Department of Mathematics, University of the Basque Country UPV/EHU,*
Barrio Sarriena s/n, E-48940 Leioa, Basque Country – Spain

[3] *Ikerbasque - Basque Foundation for Science,*
Calle de María Díaz de Haro 3, E-48013 Bilbao, Basque Country – Spain

emails: atrucchia@bcamath.org, gpagnini@bcamath.org

Abstract

In this work we study the role of a complex environment in the propagation of a front with curvature-dependent speed. The motion of the front is split into a drifting part and a fluctuating part. The drifting part is obtained by using the level set method, and the fluctuating part by a probability density function that gives a comprehensive statistical description of the complexity of the environment. In particular, the environment is assumed to be a diffusive environment characterized by the Erdélyi–Kober fractional diffusion. The evolution of the front is then analysed with a Polynomial Chaos surrogate model in order to perform Sensitivity Analysis on the parameters characterizing the diffusion and Uncertainty Quantification procedures on the modeled interface. Sparse techniques for Polynomial Chaos allowed a limited size for the simulation databases.

Key words: random front propagation – level set method – Erdélyi–Kober fractional diffusion – $\mathcal{M}$-Wright/Mainardi function – Sensitivity Analysis
MSC 2000: [2010] 35F21 – 60G22 – 60K37 – 65M08 – 49Q12

1 Introduction

Front propagation plays an important role in many fields of applied science. It might happen that the propagating interface is embedded in a medium characterized by a random motion which implies some diffusion process. In classical diffusion, the process is Gaussian and the

 ISBN: 978-84-697-7861-6

particle mean square displacement grows linearly in time. On the other hand, diffusion in complex media diffusion displays a non Gaussian density and non-linear growth in time, as for example in biological systems [1, 7] or in fluids and plasmas [4]. In these cases diffusion is labelled as *anomalous diffusion* [3, 7, 1, 22].

The aim of the present work is to analyze the role of the environment in a kinetic where there is an interplay between the geometric features of the front and the statistical characteristics of the random/complex environment.

The main items of the proposed method are:

- the *average front position* is computed by the level set method (LSM) [29];
- the probabilistic spread of the front around the average position is described by a probability density function (PDF) linked to the underlying diffusive process;
- an *effective front* emerges from the superposition of the fluctuating fronts as the weighted mean of the average fronts adopting the previously chosen PDF as a weight function.

This methodology to depict random fronts has been introduced first to study the evolution of the burnt mass fraction in turbulent premixed combustion [23], and later has been applied successfully to wild-land fire propagation simulation [24, 25, 26, 20, 21, 15]. In these two cases, the chosen PDF was either the Gaussian one [23, 24, 25, 26, 20, 21], or a convolution of the Gaussian with a lognormal PDF in relation to the specific application [26, 20, 21].

Here, the role of the enviornment is studied by using a PDF that that solve the Erdélyi–Kober fractional diffusion equation [18]: a quite general time-fractional diffusion process that depends on the parameters $0 < \alpha \leq 2$ and $0 < \beta \leq 1$ and shows sub- $(0 < \alpha < 1)$ and super-diffusion $(1 < \alpha < 2)$. The PDF is the multi-dimensional extension of the one-dimensional $\mathcal{M}$-Wright/Mainardi function that moves from the exponential $(\beta = 0)$ to the Gaussian density function $(\beta = 1)$.

The complex kinetic of the front is studied with a Polynomial Chaos surrogate model in order to perform Sensitivity Analysis (SA) and Uncertainty Quantification (UQ) procedures for parameters α and β.

The paper will have the subsequent structure: in Section 2 the modelling approach is presented and the numerical experiments are described in Section 3. In Section 4 we introduce the routines for the Surrogate-based UQ and SA. Conclusions and further research are outlined in 5.

 ISBN: 978-84-697-7861-6

2 Model

2.1 Modelling approach

The modelling approach adopted in this paper is fully presented and discussed in Refs. [26, 13, 14, 9]. This approach is based on the idea to split the motion of the front into a *drifting* part and a *fluctuating* part and the front position is also split correspondingly. In particular, the drifting part can be obtained by existing methods for simulate front propagation, for example the Eulerian LSM (or G-equation in the combustion community [17]) or the Lagrangian Discrete Event System Specification (DEVS) [5]. The fluctuating part is the result of a comprehensive statistical description of the phenomenon which includes the random effects in agreement with the physical properties of the system.

The random front line is obtained as follows. First a front contour $\Gamma(t)$ is computed by using an opportune existing method (in the present case the LSM) and this step gives the drifting part of the front position. Later a *deterministic* indicator function is introduced which takes the values 0 and 1 outside and inside the domain $\Omega(t) \subset \mathbb{R}^n$, $n \geq 1$, surrounded by the computed front contour $\Gamma(t)$. Since the front line can be re-located in a different position by using the translation or *sifting property* of the Dirac delta function, by using a delta function peaked on a random position, a *random front contour* is constructed. A *stochastic* indicator function can be determined by an integral formula involving the product of the deterministic indicator function times the Dirac delta function peaked along the stochastic trajectory. Finally, by applying the ensemble average, the averaged stochastic indicator function states the effective front position by a smooth function $\varphi_e : \mathcal{S} \times \mathbb{R}_0^+ \to [0,1]$, where $\mathcal{S} \subseteq \mathbb{R}^n$ is the domain of interest. A selected isoline/isosurface of this smooth function represents the effective front line emerging from the proposed method, i.e., $\Gamma_e(t) = \{\mathbf{x} \in \mathcal{S} | \varphi_e(\mathbf{x}, t) = \varphi_*\}$.

Let $\mathbf{x} \in \mathcal{S} \subseteq \mathbb{R}^n$ and $t \in \mathbb{R}_0^+$, in formulae we have the following indicator function $I_\Omega : \mathcal{S} \times \mathbb{R}_0^+ \to \{0,1\}$ defined as

$$I_\Omega(\mathbf{x}, t) = \begin{cases} 1\,, & \mathbf{x} \in \Omega(t) \\ \\ 0\,, & \text{elsewhere} \end{cases}, \tag{1}$$

where $\Omega(t)$ is the domain surrounded by the frontline generated at time t by the adopted operational code. Let $\mathbf{X}^\omega(t, \overline{\mathbf{x}}) = \overline{\mathbf{x}} + \xi_t^\omega$ be the ω-realization of a stochastic trajectory where $\overline{\mathbf{x}}$ is a point inside the domain $\Omega(t)$ established at time t by the adopted operational code and ξ_t is the random noise. The one-particle density function of $\mathbf{X}^\omega(t, \overline{\mathbf{x}})$ is $p^\omega(\mathbf{x}; t|\overline{\mathbf{x}}) = \delta(\mathbf{x} - \mathbf{X}^\omega(t, \overline{\mathbf{x}}))$ and, after the ensemble averaging denoted here by $\langle \cdot \rangle$, the PDF of $\mathbf{X}^\omega(t, \overline{\mathbf{x}})$ results to be $p(\mathbf{x}; t|\overline{\mathbf{x}}) = \langle \delta(\mathbf{x} - \mathbf{X}^\omega(t, \overline{\mathbf{x}})) \rangle$. The indicator function $I_\Omega(\mathbf{x}, t)$ turns to be stochastic by using the sifting property of the delta function as explained above, i.e.,

$$I_\Omega^\omega(\mathbf{x}, t) = \int_{\mathcal{S}} I_\Omega(\overline{\mathbf{x}}, t) \delta(\mathbf{x} - \mathbf{X}^\omega(t, \overline{\mathbf{x}}))\, d\overline{\mathbf{x}}\,. \tag{2}$$

 ISBN: 978-84-697-7861-6

Finally, after ensemble averaging of $I^{\omega}_{\Omega}(\mathbf{x},t)$ it follows

$$\begin{aligned}\langle I^{\omega}_{\Omega}(\mathbf{x},t)\rangle &= \langle \int_{\mathcal{S}} I_{\Omega}(\overline{\mathbf{x}},t)\delta(\mathbf{x}-\mathbf{X}^{\omega}(t,\overline{\mathbf{x}}))\,d\overline{\mathbf{x}}\rangle = \int_{\mathcal{S}} I_{\Omega}(\overline{\mathbf{x}},t)\langle\delta(\mathbf{x}-\mathbf{X}^{\omega}(t,\overline{\mathbf{x}}))\rangle\,d\overline{\mathbf{x}} \\ &= \int_{\mathcal{S}} I_{\Omega}(\overline{\mathbf{x}},t)p(\mathbf{x};t|\overline{\mathbf{x}})\,d\overline{\mathbf{x}} = \int_{\Omega(t)} p(\mathbf{x};t|\overline{\mathbf{x}})\,d\overline{\mathbf{x}} = \varphi_e(\mathbf{x},t)\,. \end{aligned} \tag{3}$$

The averaging procedure can pass into the integral because the domain of integration is not affected by the stochastic motion and the indicator function $I_{\Omega}(\overline{\mathbf{x}},t)$ comes out of the averaging brackets because it is a deterministic quantity.

Some remarks on the above method are:

i) if a non-random initial front contour is considered, the initial condition of the PDF of fluctuations is a Dirac delta function;

ii) if no randomness occurs in the process, the PDF of fluctuations remains a Dirac delta function so the result of the proposed method reduces to the chosen literature method (e.g., LSM or DEVS);

iii) the proposed method avoids to use the Reynolds decomposition of the value of the observable function, as it was erroneously assumed sometimes in literature in the context of turbulent premixed combustion in terms of the G-equation [27, 28, 10]. In fact, by definition, the curve representing the frontline does not have fluctuations in its value in any adopted method, but it has fluctuations in its position and these fluctuations are exactly what is modelled in the present method by the fluctuating part and its PDF.

iv) the resulting effective front differs from the front that follows from the averaging procedure proposed by Oberlack et al. [17], because in the method proposed here the full PDF is considered, which means that the variance of interface position is also included, along with the average position. This difference is fundamental to take into account the diffusive characteristics, the displacement variance being closely related to velocity correlation, i.e., Green–Kubo–Taylor formula, which is the most important element to characterize the structure of stochastic processes. If the displacement variance tends to zero, then the PDF tends to the Dirac delta function and the averaged G-equation derived by Oberlack et al. [17] is recovered.

2.2 Determination of the drifting part

In this study we consider the LSM for the drifting part.

Let $\gamma : \mathcal{S}\times\mathbb{R}^{+}_{0}\to\mathbb{R}$, then its evolution in the framework of the LSM is governed by the following Hamilton–Jacobi equation

$$\frac{\partial\gamma}{\partial t} = \mathcal{V}(\mathbf{x},t)\,\|\nabla\gamma\|. \tag{4}$$

 ISBN: 978-84-697-7861-6

The domain $\Omega(t)$ is that one bounded by the front contour $\Gamma(t)$ now established by the level set value $\gamma(\mathbf{x},t)=\gamma_*$, i.e., $\Gamma(t)=\{\mathbf{x}\in\mathcal{S}|\gamma(\mathbf{x},t)=\gamma_*\}$.

When the speed of the front depends on the curvature, Equation (4) with a curvature-dependent speed reads

$$\frac{\partial\gamma}{\partial t}=\mathcal{V}_0(1-\lambda\kappa(\mathbf{x},t))\,\|\nabla\gamma\|\,, \tag{5}$$

where κ is the curvature of the front, i.e.,

$$\kappa(\mathbf{x},t)=\nabla\cdot\left(\frac{\nabla\gamma(\mathbf{x},t)}{\|\nabla\gamma(\mathbf{x},t)\|}\right)\,, \tag{6}$$

$\mathcal{V}_0$ is a drifting speed here assumed constant and λ is the scale of the front curvature. In combustion literature, λ is called Markstein length.

By including the curvature, the mathematical problem passes from hiperbolic to parabolic. This transition could affect the evolution of the front by provoking for example a quenching behaviour.

2.3 Determination of the fluctuating part

The PDF of fluctuations can be derived from the analysis of the physics of the system. So in the case of classical diffusive environments it is Gaussian while it can be a more general PDF when anomalous diffusion occurs, e.g., [18, 22].

The generalized diffusion process here considered is the isotropic multi-dimensional Erdélyi–Kober fractional diffusion [18], and its Green function is the PDF $p(\mathbf{x};t)$ to plug into in Eq. (3). The associated stochastic process is called generalized grey Brownian motion (ggBm) [16]. To deal with multi-dimensionality, by using an integral representation formula of the one-dimensional $\mathcal{M}$-Wright/Mainardi function [12], Green function for multi-dimensional cases can be represented by the same integral formula of by using the multi-dimensional Gaussian PDF [13]. The desired PDF is

$$\begin{aligned} p(\mathbf{x};t) &= \int_0^\infty \frac{\mathrm{e}^{-\|\mathbf{x}\|^2/(4D\tau)}}{(4\pi D\tau)^{n/2}}\,\mathcal{M}_\beta\left(\frac{\tau}{t^\alpha}\right)\,\frac{d\tau}{t^\alpha} = \int_0^\infty \prod_{i=1}^n \frac{\mathrm{e}^{-x_i^2/(4D\tau)}}{(4\pi D\tau)^{1/2}}\,\mathcal{M}_\beta\left(\frac{\tau}{t^\alpha}\right)\,\frac{d\tau}{t^\alpha} \\ &= \int_0^\infty \prod_{i=1}^n \frac{\mathrm{e}^{-x_i^2/(4D\lambda t^\alpha)}}{(4\pi D\lambda t^\alpha)^{1/2}}\,\mathcal{M}_\beta(\lambda)\,d\lambda = \frac{1}{(Dt^\alpha)^{n/2}}\,\mathbb{M}_{\beta/2}\left(\frac{\|\mathbf{x}\|}{\sqrt{Dt^\alpha}}\right)\,, \end{aligned} \tag{7}$$

where the notation $\mathbb{M}_\eta(z)$ is used for the multi-dimensional extension of the $\mathcal{M}$-Wright/Mainardi function $\mathcal{M}_\eta(z)$ [11, 19]. The main outcomes of this modelling choice is the clear separation between the shape of the PDF and the variance of the underlying stochastic process because they are controlled by two independent parameters.

The fact that the diffusive regimes (wheter it happens to be super or sub-diffusive) is up to the α parameter is highlighted by the particle variance σ_d^2 which in one–, two– and

 ISBN: 978-84-697-7861-6

three–dimensions ($d = 1, 2, 3$) is [6]:

$$\sigma_1^2 = \int_{-\infty}^{+\infty} x^2\, p(x;t)\, dx = \frac{2D\, t^{\alpha}}{\Gamma(\beta+1)}, \qquad \sigma_2^2 = 2\,\sigma_1^2, \qquad \sigma_3^2 = 3\,\sigma_1^2. \tag{8}$$

Differently from the analysis performed in [13, 14], the PDF stated in (7) allows for studying indpendently the spreading (driven by α) and the shape of the PDF (driven by β).

3 Numerical results

A series of numerical experiments are conducted to study the motion of the front under the effects of the curvature and the statistical characterization of the complex environment.

The computational domain is a square box, with side of $1\,a.u.$, and the radius of the initial circle is $0.2\,a.u.$. In order to highlight the dependence of the front evolution on its geometry, a particular initial shape $\gamma^*(t=0)$ is chosen. Such initial front is given by a circle from which 4 equally space rectangles are carved only in the upper part. The horizontal length of each rectangle is $0.04\,a.u.$. The resulting front display an hand-shape profile. The motion smears out the sharp angles and the front exhibits a uniform curvature in the lower half part and a heterogeneous curvature in the upper one.

The front evolution exhibits a rich behaviour, initial condition and a glimpse on the evolution are shown in Figure 1a,b. The main role of each parameter is briefly reported:

1. The *normal velocity* in the lower part of the hand-shaped contour advects the $\gamma = 0$ iso-contour along a radial direction. In the upper part, the same occurs for the outer part of the fingers. The inner sides of the fingers is advected, one towards the other, by the normal velocity and the bigger the value of V_0, the less the deterministic shape of the front mantains its characteristic form before collapsing into a circle.

2. The curvature effect (governed in this case by λ) contributes to smear out the disuniformities of the initial profile, by contributing to the convergence to a circle. Its effect is of paramount importance in the upper part of the hand-shaped profile, becasue the radius of curvature is significantly smaller in the corners of the fingers, while in the lower side the radius of curvature is larger and uniform.

3. The diffusion coefficient D of the PDF governs the sharpness of the effective indicator φ_e (the higher ν, the less sharp the φ_e profile). It plays an important role on the eventual shrinking of the $\varphi_e = \varphi_{th}$ iso-contour [13]. We remark the limit

$$\lim_{D\to 0} p(\mathbf{x};t) = \delta(\mathbf{x};t)\,, \tag{9}$$

that gives an intuitive explanation that the iso-contours of φ_e eventually stick to the deterministic front when D is low.

 ISBN: 978-84-697-7861-6

4. The parameters α and β control the sub- and super-diffusion and the deviation from the Gaussianity, respectively. Their role in the evolution of the front is investigated by the means of SA and UQ procedures in Section 4.

4 Surrogate-Based Sensitivity Analysis and Uncertainty Quantification

The investigated front exhibits puzzling results on its evolution, mainly due to the effects of the parameters α, β on the effective indicator φ_e. In order to measure explicitly some observable of the evolution of equations (4) and (3) we define as Quantities of Interest (QoI) the area surrounded by the contour $\varphi_{th} = 0.5$ at time $t = T$, i.e.,

$$Y(T) = \frac{1}{A} \int_{\varphi(\mathbf{x}) > \varphi_{th}} \mathbf{1} d\mathbf{x} \,, \tag{10}$$

where A is the area of the computational domain. For our purposes, the map $[0, 2] \times [0, 1] \to \mathbb{R}^+$ that links a choice of the parameters α, β with a shape configuration for φ_e and ultimately to a QoI $Y(T)$ has to be studied. To order the input parameters by their relevance, as well as to quantify their effects accounting or not the interaction with the others, a Variance-Based Sensitivity Analysis is seeked, in order to obtain the so-called Partial and Total Sobol' Indices [30, 8]. By assuming Uniform PDFs $\mathcal{U}[0, 2]$ and $\mathcal{U}[0, 1]$, statistical quantities on such QoI can be derived through UQ procedures. Since the number of simulations to achieve both objectives is too demanding to be fulfilled through Montecarlo simulations, a Surrogate Model is implemented to mimick the evolution of the system and construct a cheap-to-evaluate function that is the closest possible to the one given by the numerical implementation of the model. In order to do so, Polynomial Chaos Surrogate [31] is employed. The main idea of this approach is to design the mimicked QoI Y with a weighted finite sum of basis functions:

$$\widehat{Y}\,(\mathbf{p}) = \sum_{i=0}^{r} \gamma_i \, \Psi_i \,(\mathbf{p}) \,, \tag{11}$$

where $\mathbf{p}$ is the vector of input parameters, while the coefficients γ_i and the basis functions Ψ_i are calibrated by a training set $\mathcal{D}_{NDOE}$ contructed from a series of simulations. For PC expansion, the maximum order of the decomposition and the basis functions are first chosen, then projection strategy is implemented to compute the decomposition coefficients in the polynomial basis. The main steps of the adopted procedure are:

1. Sample $N_{DOE} = 216$ points $\mathbf{p} = \{\alpha, \beta\}_k$ using the low-discrepancy Halton method. Construct the Design of Experiment, i.e., the database $\mathcal{D}_{NDOE} = (\mathbf{p}_k, Y(\mathbf{p}_k))_{k=1...N_{DOE}}$.

 ISBN: 978-84-697-7861-6

2. Construct a Polynomial Chaos surrogate $\mathfrak{M}$ with sparse strategy for basis selection LAR [2].

3. Computation of the Leave-One-Out cross-validation error to estimate the goodness of $\mathfrak{M}$.

4. Study of sensitivity analysis via Sobol' Indices computed via the coefficients of the PC expansion γ_i .

5. Uncertainty quantification of the output Y given uncertainties on the input parameters.

In order to study α and β only, the rest of parameters is fixed to nominal values. More specifically, $D = 100$, $\lambda = 0.1$, $V_0 = 1$. The QoI is estimated at $T = 1$. Main results are shown in Figure 1c,d,e,f.

5 Conclusions

In this paper we study the propagation of an interface embedded in a complex environment characterised by anomalous diffusion. We considered a non-circular front, whose interface is moved by the LSM with a velocity dependent on the front curvature, and the anomalous diffusion is modelled through a non-Gaussian PDF that is the solution of a fractional diffusion equation in the Erdélyi–Kober sense. We study the kinetic of the front where the interplay between geometric and stochastic features act. The geometric features are represented by the outward normal velocity of the front in the case of a curvature-independent speed and by the length-scale of the curvature. The stochastic features are represented by a first parameter α controlling the exponent of the power-law governing the growing in time of the variance of the fluctuation PDF and a second parameter β controlling the deviation from the Gaussian density of the PDF of fluctutions of the front position.

We studied the role of the parameters characterizing the anomalous diffusion by performing a sensitivity analysis through a PC-aided sensitivity Analysis. A good value for LOO error is reached by the PC surrogate ($< 10^{-4}$), and the SA shows the greater relevance of α in comparison with β, even though both actors play a role on the QoI Y. The difference from partial and total Sobol' Indices represents an interaction between the two parameters. In particular, we observe through the Sobol' Indices that the parameter governing the aforementioend power-law plays a prominent role in quantifying the area enclosed by the front, but neither the other parameter nor the interactions between the two can be completely neglected.

The next step of the research is the implementation of a Gaussian Process Surrogate for a comparison with the PC method, as well as the simultaneous study of the role of all the involved parameters, to highlight the benefits of sparse techniques for PC.

 ISBN: 978-84-697-7861-6

Acknowledgements

This research is supported by the Basque Government through the BERC 2018–2021 program and by Spanish Ministry of Economy and Competitiveness MINECO through BCAM Severo Ochoa excellence accreditation SEV-2013-0323 and through project MTM2016-76016-R "MIP" and by the PhD grant "La Caixa 2014".

References

[1] E. Barkai, Y. Garini, and R. Metzler, *Strange kinetics of single molecules in living cells*, Phys. Today, 65 (2012), pp. 29–35.

[2] G. Blatman and B. Sudret, *Adaptive sparse polynomial chaos expansion based on least angle regression*, J. Comput. Phys., 230 (2011), pp. 2345–2367.

[3] A. Blumen, A. A. Gurtovenko, and S. Jespersen, *Anomalous diffusion and relaxation in macromolecular systems*, J. Non-Cryst. Solids, 305 (2002), pp. 71–80.

[4] D. del Castillo-Negrete, *Non-diffusive, non-local transport in fluids and plasmas*, Nonlin. Processes Geophys., 17 (2010), pp. 795–807.

[5] J. B. Filippi, F. Morandini, J. H. Balbi, and D. Hill, *Discrete event front tracking simulator of a physical fire spread model*, Simulation, 86 (2010), pp. 629–646.

[6] A. Hanyga, *Multidimensional solutions of time-fractional diffusion-wave equations*, Proc. R. Soc. Lond. A, 458 (2002), pp. 933–957.

[7] F. Höfling and T. Franosch, *Anomalous transport in the crowded world of biological cells*, Rep. Prog. Phys., 76 (2013), p. 046602.

[8] B. Iooss and A. Saltelli, *Introduction to sensitivity analysis.*, Handbook of Uncertainty Quantification, (2016), pp. 1 – 20.

[9] I. Kaur, A. Mentrelli, F. Bosseur, J.-B. Filippi, and G. Pagnini, *Turbulence and fire-spotting effects into wild-land fire simulators*, Commun. Nonlinear Sci. Numer. Simul., 39 (2016), pp. 300 – 320.

[10] A. N. Lipatnikov and V. A. S. V.A., *Some basic issues of the averaged G-equation approach to premixed turbulent combustion modeling*, Open Thermodyn. J., 2 (2008), pp. 53–58.

[11] F. Mainardi, A. Mura, and G. Pagnini, *The M-Wright function in time-fractional diffusion processes: A tutorial survey*, Int. J. Diff. Equations, 2010 (2010), p. 104505.

 ISBN: 978-84-697-7861-6

[12] F. Mainardi, G. Pagnini, and R. Gorenflo, *Mellin transform abd subordination laws in fractional diffusion processes*, Fract. Calc. Appl. Anal., 6 (2003), pp. 441–459.

[13] A. Mentrelli and G. Pagnini, *Front propagation in anomalous diffusive media governed by time-fractional diffusion*, J. Comput. Phys., 293 (2015), pp. 427–441.

[14] ——, *Random front propagation in fractional diffusive systems*, Commun. Appl. Ind. Math., 6 (2015), pp. e–504.

[15] ——, *Modelling and simulation of wildland fire in the framework of the level set method*, Ricerche Mat., 65 (2016), pp. 523–533.

[16] A. Mura and G. Pagnini, *Characterizations and simulations of a class of stochastic processes to model anomalous diffusion*, J. Phys. A: Math. Theor., 41 (2008), p. 285003.

[17] M. Oberlack, H. Wenzel, and N. Peters, *On symmetries and averaging of the g-equation for premixed combustion*, Combust. Theory Modelling, 5 (2001), pp. 363–383.

[18] G. Pagnini, *Erdélyi–Kober fractional diffusion*, Fract. Calc. Appl. Anal., 15 (2012), pp. 117–127.

[19] ——, *The M-Wright function as a generalization of the Gaussian density for fractional diffusion processes*, Fract. Calc. Appl. Anal., 16 (2013), pp. 436–453.

[20] ——, *A model of wildland fire propagation including random effects by turbulence and fire spotting*, in Proceedings of XXIII Congreso de Ecuaciones Diferenciales y Aplicaciones XIII Congreso de Matemática Aplicada. Castelló, Spain, 9–13 September 2013, 2013, pp. 395–403.

[21] ——, *Fire spotting effects in wildland fire propagation*, in Advances in Differential Equations and Applications, F. Casas and V. Martínez, eds., vol. 4 of SEMA SIMAI Springer Series, Springer International Publishing Switzerland, 2014, pp. 203–216. ISBN: 978-3-319-06952-4. (eBook: 978-3-319-06953-1).

[22] ——, *Short note on the emergence of fractional kinetics*, Physica A, 409 (2014), pp. 29–34.

[23] G. Pagnini and E. Bonomi, *Lagrangian formulation of turbulent premixed combustion*, Phys. Rev. Lett., 107 (2011), p. 044503.

[24] G. Pagnini and L. Massidda, *Modelling turbulence effects in wildland fire propagation by the randomized level-set method*, Tech. Rep 2012/PM12a, CRS4, July 2012. Revised Version August 2014. arXiv:1408.6129.

 ISBN: 978-84-697-7861-6

[25] ——, *The randomized level-set method to model turbulence effects in wildland fire propagation*, in Modelling Fire Behaviour and Risk. Proceedings of the International Conference on Fire Behaviour and Risk. ICFBR 2011, Alghero, Italy, October 4–6 2011, D. Spano, V. Bacciu, M. Salis, and C. Sirca, eds., May 2012, pp. 126–131. ISBN 978-88-904409-7-7.

[26] G. Pagnini and A. Mentrelli, *Modelling wildland fire propagation by tracking random fronts*, Nat. Hazards Earth Syst. Sci., 14 (2014), pp. 2249–2263.

[27] N. Peters, *A spectral closure for premixed turbulent combustion in the flamelet regime*, J. Fluid Mech., 242 (1992), pp. 611–629.

[28] ——, *The turbulent burning velocity for large-scale and small-scale turbulence*, J. Fluid Mech., 384 (1999), pp. 107–132.

[29] J. A. Sethian and P. Smereka, *Level set methods for fluid interfaces*, Ann. Rev. Fluid Mech., 35 (2003), pp. 341–372.

[30] I. Sobol, *Sensitivity analysis for nonlinear mathematical models*, Math. Modeling Comput. Experiment, 1 (1993), pp. 407–414.

[31] D. Xiu and G. Karniadakis, *The wieneraskey polynomial chaos for stochastic differential equations*, SIAM J. Sci. Comput., 24 (2002), pp. 619–644.

 ISBN: 978-84-697-7861-6

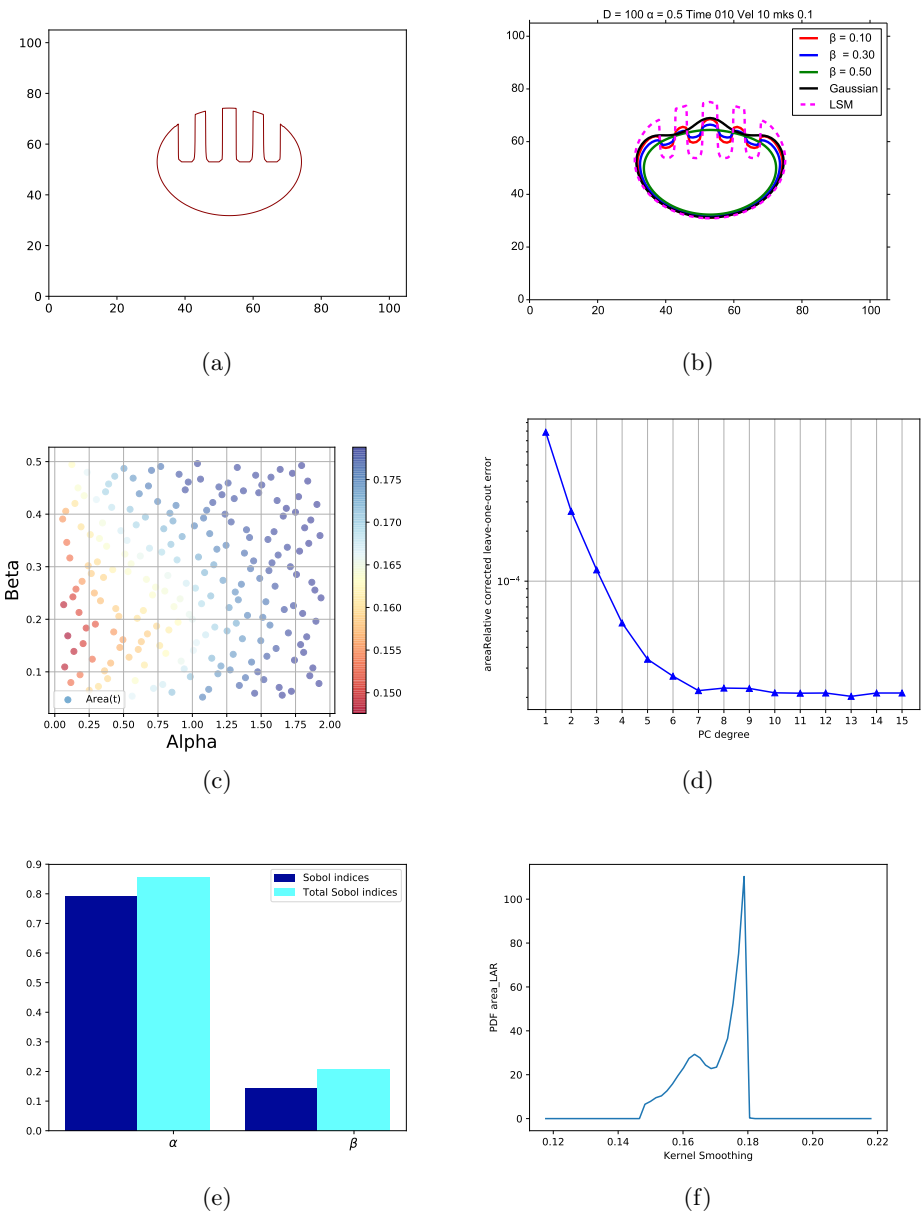

Figure 1: Panel: (a) initial configuration of γ^*; (b) contours of φ_{th} with different values of β and $\alpha = 0.5$ and $\alpha = 1$ corresponding to the Gaussian PDF; (c) DOE colored by the value of Y on the sampling points; (d) LOO error over the maximum polynomial degree for LAR; (e) the Partial (Dark Blue) and Total (Light Blue) Sobol' Indices for α and β; (f) the PDF of Y assuming random configuration for α and β.

ISBN: 978-84-697-7861-6